Adjustable-Speed Single-Phase IM Drive with Reduced Number of Switches

Miroslav Chomat, *Member, IEEE*
Institute of Electrical Engineering
Czech Academy of Sciences
Dolejskova 5, 182 02 Prague
Czech Republic

Thomas A. Lipo, *Fellow, IEEE*
Department of Electrical and Computer Engineering
University of Wisconsin-Madison
1415 Engineering Drive
Madison, WI 53706, USA

***Abstract*-A novel low-cost single-phase induction machine drive containing only two controlled solid-state switches is presented. The drive is intended for an HVAC type of application requiring variable-speed operation. An experimental drive based on the proposed setup has been developed and built to verify its practical viability and properties. The paper presents the results obtained from an investigation into this new topology and discusses the properties and characteristics of the drive for the entire speed range from 0 to 60 Hz.**

I. INTRODUCTION

Large portions of electrical energy produced in developed countries are consumed for heating, ventilation, and air conditioning (HVAC) in residential areas and for similar applications in the industrial sphere. At present, most of these applications, especially those with lower nominal power, utilize fixed-speed drives and their regulation is achieved primarily by throttling the output flow of the media [1]. Therefore, there is a great potential for energy savings if one manages to introduce energy efficient variable-speed drives into these areas on a massive scale. The problem, however, lies in generally much higher prices for conventional variable-speed drives compared to fixed-speed ones, which is the reason why so much attention has recently been paid to unconventional drive setups with reduced number of solid-state switches [2, 3] or to drives using cheaper to manufacture single-phase machines [4-8].

This paper focuses on properties of a drive that uses a single-phase machine of permanent-split capacitor type to drive a fan-type load with variable mechanical speed. To generate the supply voltage with variable frequency a converter with the minimal number of active switches and diodes is used. Such a system cannot fully satisfy requirements of dynamically demanding applications, but could represent a technically and economically viable solution for HVAC or other similar applications.

II. SYSTEM DESCRIPTION

A simplified scheme of the considered system is in Fig. 1. A front-end voltage doubler is connected to a single-phase supply. The output portion of the converter consisting of two IGBT or MOSFET switches generates a pulse width modulated (PWM) output supplying one or both stator windings of a single-phase machine. The single-phase machine is considered of the permanent-split capacitor type with the main and auxiliary windings of generally different number of turns. According to the position of the relay contacts at the output of the inverter, one of two principal modes of operation may be selected. These modes are the full-speed mode (position 1) and the variable-speed mode (position 2).

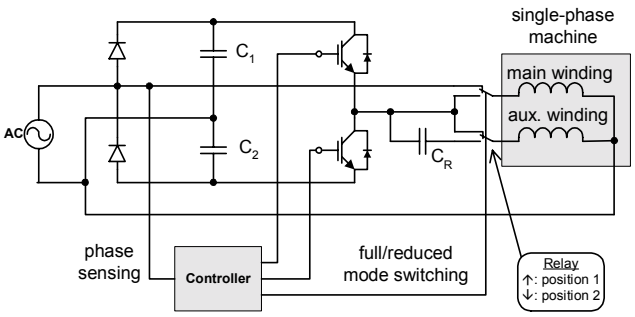

Fig. 1. Scheme of system under investigation.

In the full-speed mode, the main winding is connected directly to the mains and is, therefore, supplied with voltage of the nominal network frequency and amplitude. The inverter produces voltage for the auxiliary winding with the same frequency. The amplitude and the phase of this voltage in respect to the mains are adjusted with the semiconductor switches so that the optimal operation of the machine is achieved.

The variable-speed operation is characterized by the fact that both stator windings are fed from the inverter. The phase shift between the currents in the main and auxiliary windings of the machine is maintained by means of an AC capacitor connected in series with the auxiliary winding. The frequency of the supply voltage can be continuously varied from zero to the nominal frequency of the mains and the mechanical speed of the machine varies accordingly.

The generation of the triggering pulses for the solid-state switches and the state of the output relay are controlled by a single-chip microcontroller. For correct function of the drive in the full-speed mode, it is necessary to synchronize the inverter output with the mains and, therefore, phase sensing of the mains voltage needs to be implemented in the controller.

III. MATHEMATICAL MODEL

A numerical model of the considered system has been developed based on the mathematical description of a single-

phase induction machine. The electrical machine being considered may be described by the following set of ordinary differential equations in the stator reference co-ordinate frame under the commonly used simplifying assumptions.

$$u_{S\alpha} = R_{S\alpha} i_{S\alpha} + L_{S\alpha} \frac{di_{S\alpha}}{dt} + L_{M\alpha} \frac{di_{R\alpha}}{dt} \quad (1)$$

$$u_{S\beta} = R_{S\beta} i_{S\beta} + L_{S\beta} \frac{di_{S\beta}}{dt} + L_{M\beta} \frac{di_{R\beta}}{dt} \quad (2)$$

$$0 = R_{R\alpha} i_{R\alpha} + L_{R\alpha} \frac{di_{R\alpha}}{dt} + L_{M\alpha} \frac{di_{S\alpha}}{dt} + \frac{1}{a} \omega_m \left(L_{R\beta} i_{R\beta} + L_{M\beta} i_{S\beta} \right) \quad (3)$$

$$0 = R_{R\beta} i_{R\beta} + L_{R\beta} \frac{di_{R\beta}}{dt} + L_{M\beta} \frac{di_{S\beta}}{dt} - a \omega_m \left(L_{R\alpha} i_{R\alpha} + L_{M\alpha} i_{S\alpha} \right) \quad (4)$$

where

$$a = \frac{N_{S\beta}}{N_{S\alpha}} \quad (5)$$

is the ratio between the effective numbers of turns in the auxiliary and the main stator windings. Subscript α denotes variables in the main winding and subscript β denotes variables in the auxiliary winding. Parameters and quantities with subscripts *S* and *R* are those in the stator and the rotor respectively. The rotor parameters are referred to the stator. Mechanical speed ω_m is in electrical degrees.

The instantaneous electromagnetic torque produced is then given by equation

$$T_e = p \left[a \left(L_{M\alpha} i_{S\alpha} + L_{R\alpha} i_{R\alpha} \right) i_{R\beta} - \frac{1}{a} \left(L_{M\beta} i_{S\beta} + L_{R\beta} i_{R\beta} \right) i_{R\alpha} \right] \quad (6)$$

where *p* is the number of pole pairs.

These equations can be directly used to represent the machine in a dynamic Simulink model of the system and can also serve as a starting point for derivation of a phasor model for computing steady-state characteristics. In some cases, a double revolving field theory has also been used in the analysis [9, 10].

The full-speed mode operation of this drive has been discussed in detail in [11]. Therefore, it is not addressed in detail here. Rather, this paper focuses on variable-speed operation.

IV. Variable-Speed Operation

In the variable-speed mode, the machine is operated in the same manner as a fixed capacitor machine. That is, the supply frequency is not fixed and may be varied in a certain range. The choice of the optimal value of the capacitance is not as straightforward as in the case of the constant supply frequency. The optimal operation can now be achieved just in one operating point and for the other combinations of frequency and speed the currents will not be in exact quadrature, which gives rise to torque pulsations.

All the following results have been computed for a practical single-phase machine designed for a fan-type application. The parameters of the machine are in Table 1.

First, the behavior of the machine supplied by voltages of various frequencies and with different capacitor sizes applied in series with the auxiliary winding were investigated. The following figures show the characteristics for supply frequencies 15, 30, 45, and 60 Hz and capacitances 10, 20, and 30 μF. The magnitude of the supply voltage was adjusted in direct proportion to the supply frequency.

Figs. 2 to 4 correspond to operation with a capacitor value of 10 μF, which is the recommended value for the machine operating under normal conditions at 60 Hz supply frequency. The torque-speed characteristics are shown in Fig. 2 together with the assumed load torque characteristic. The load is a fan-type with a square dependence of torque on speed. It may be noted that the machine can drive the load at all chosen supply frequencies. Fig. 3 shows what torque pulsations develop in this case. The amplitude of these pulsations is plotted against the mechanical speed for different supply frequencies and can be compared again with the corresponding load torque characteristic. The minimum of these pulsations for particular supply frequencies takes place near the operating point of the machine. The amplitudes of the stator and rotor currents in the machine are shown in Fig. 4. The corresponding supply frequency may be identified from the maximum mechanical speed achieved. A significant difference between the currents in the main and the auxiliary windings should be noticed.

For the second investigation a capacitor of 20 μF was selected and larger electromagnetic torques were achieved. Torque pulsations were reduced for all the tested supply frequencies. These results are presented in Figs. 5 and 6. The machine now operates with virtually zero pulsations for a supply frequency of 60 Hz and 1050 rpm. On the other hand, from Fig. 7 it is evident that the currents in the main winding are much larger in this case.

The last set of characteristics in Figs. 8 through 10 was computed for a capacitor of 30 μF. The optimal operating point now shifts towards lower frequencies and speeds. The starting torques increase, but this is accompanied by a sharp rise in torque pulsations. The currents in the main windings also exceed their nominal values. Hence, while such a capacitor might be used as a starting capacitor for this machine, it does not appear to be very suitable as a run capacitor.

The optimal value of the capacitance in series with the auxiliary winding may be evaluated from the double revolving field theory. The resulting values for the supply

TABLE I
MOTOR RATING AND PARAMETERS

Power:	¾ h.p.	R_{1m}	9 Ω
Voltage:	230 V	R_{1a}	22 Ω
Frequency:	60 Hz	R_2	10 Ω
Speed:	1110 rpm	L_{1m}	390 mH
Aux/Main turns ratio:	1.37	L_{1a}	730 mH
Run capacitor:	10 μF	p	6

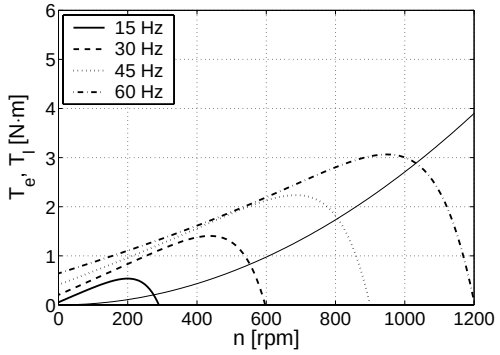

Fig. 2. Torque-speed characteristics, C = 10 μF.

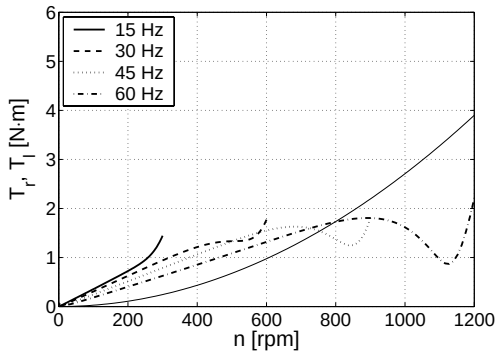

Fig. 3. Torque ripple amplitudes, C = 10 μF.

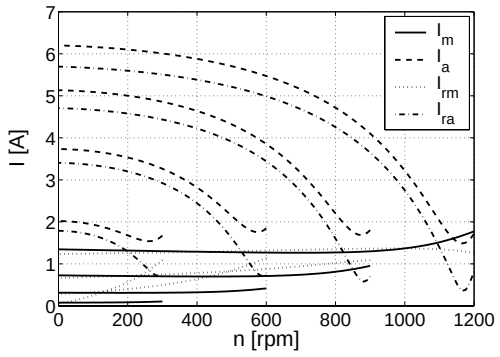

Fig. 4. Stator and rotor currents, C = 10 μF.

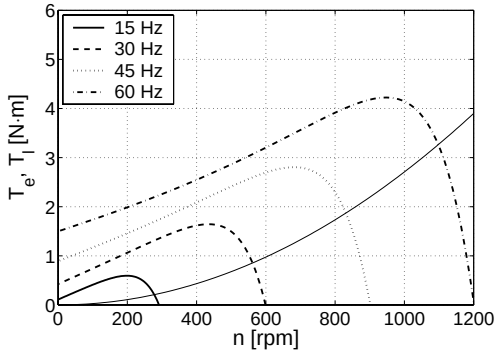

Fig. 5. Torque-speed characteristics, C = 20 μF.

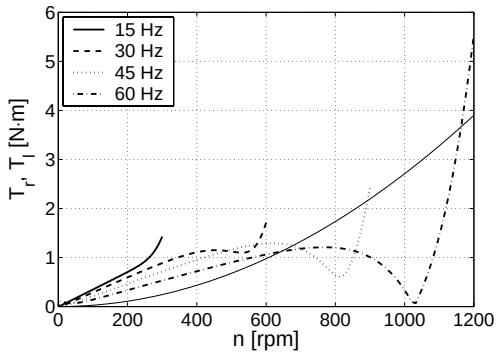

Fig. 6. Torque ripple amplitudes, C = 20 μF.

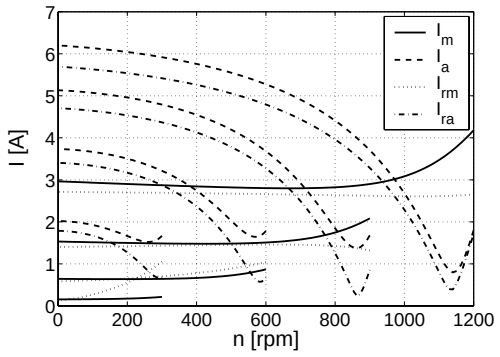

Fig. 7. Stator and rotor currents, C = 20 μF.

frequency in the range from 10 to 60 Hz are in Fig. 11. The characteristics for two different values of slip, 2.5 % and 10 % are presented. The results obtained agree with those in the preceding graphs. There is not much difference between the two considered slips. The difference would be more significant for higher values of slip. The optimum value of capacitance may not entirely compensate for the torque pulsations in all cases and additional resistances in the main or in the auxiliary winding might be required.

The dependence of the breakdown torque on the supply frequency and the series capacitance is shown in Fig. 12. The constant voltage-to-frequency ratio was maintained and the slip was considered to have a constant value of 7.5 %. The operating point with the maximal breakdown torque may not be the optimal operating point in practice as the torque pulsations could impair operation of the machine in some cases.

In variable-speed operation, the mechanical speed of the machine adjusts itself so that a balance between the electromagnetic torque and the load torque is achieved for a given supply frequency. First, a series capacitance of 10 μF was considered. Fig. 13 shows the electromagnetic torque and the amplitude of torque pulsations as functions of mechanical speed. Corresponding current amplitudes are in Fig. 14. The slip varied with speed according to the graph in Fig. 15.

Operation with a capacitor of 20 μF is illustrated in Figs. 16 through 18. The torque pulsations have a more salient local minimum at a mechanical speed of about

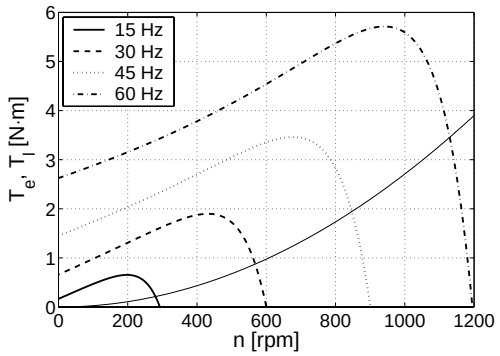

Fig. 8. Torque-speed characteristics, C = 30 μF.

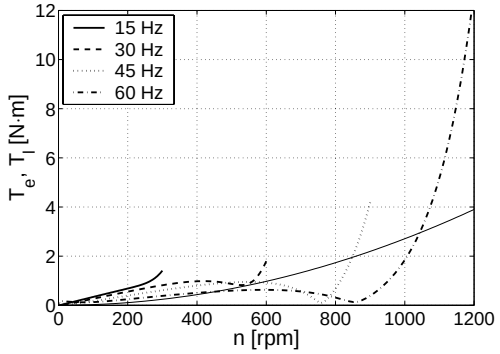

Fig. 9. Torque ripple amplitudes, C = 30 μF.

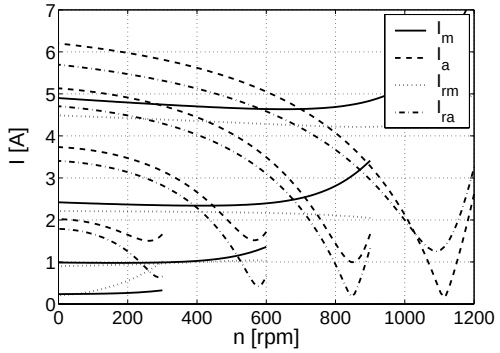

Fig. 10. Stator and rotor currents, C = 30 μF.

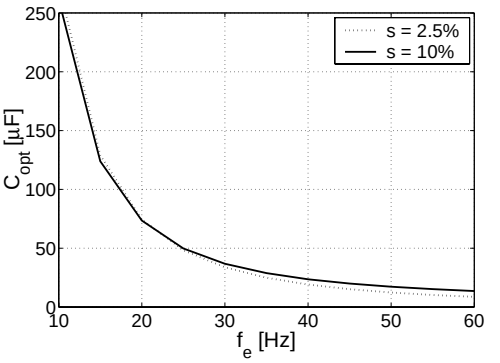

Fig. 11. Optimal run-capacitor capacitance.

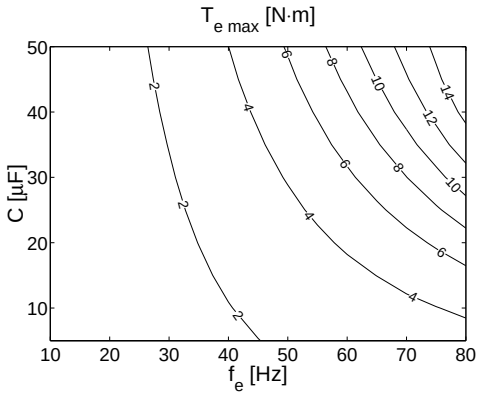

Fig. 12. Breakdown torque dependence for slip = 7.5 %.

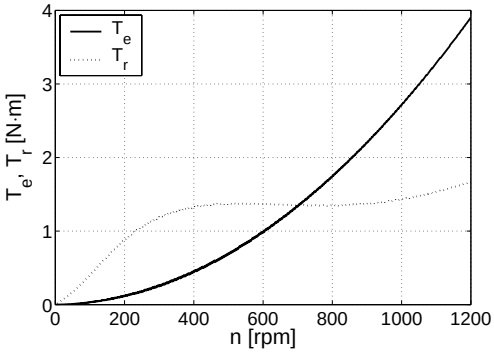

Fig. 13. Electromagnetic torque and torque ripple amplitude, C = 10 μF.

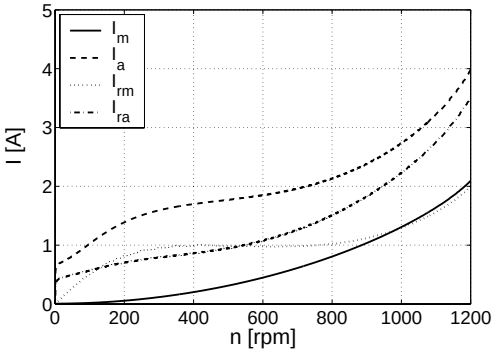

Fig. 14. Stator and rotor currents, C = 10 μF.

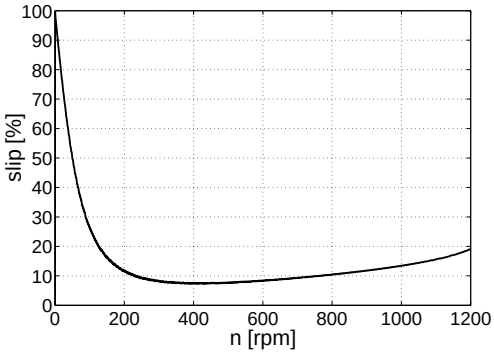

Fig. 15. Slip of machine, C = 10 μF.

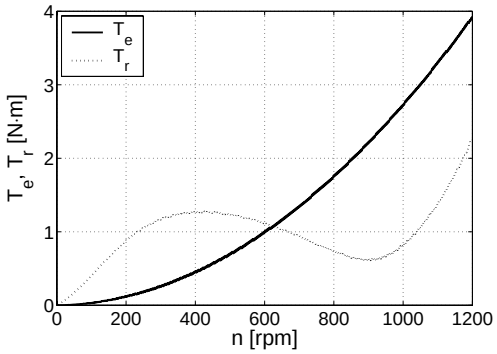

Fig. 16. Electromagnetic torque and torque ripple amplitude, C = 20 μF.

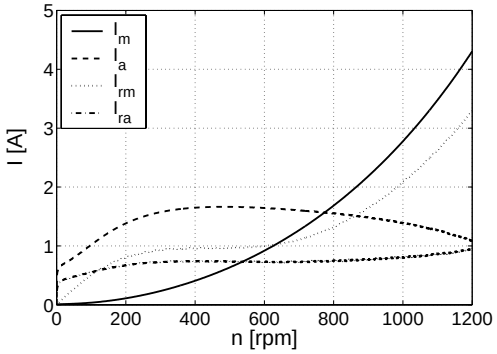

Fig. 17. Stator and rotor currents, C = 20 μF.

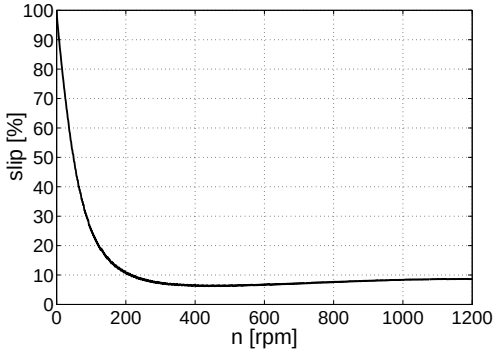

Fig. 18. Slip of machine, C = 20 μF.

900 rpm. The slip is nearly constant above 300 rpm and lies between 7 and 10 %.

The torque pulsations in operation with capacitance 30 μF would go sharply up at higher speeds and would exceed the value of the produced electromagnetic torque for most part of the speed range considered. This might cause serious problems in practice and, therefore, the characteristics are not presented here.

From these results, a capacitor of 20 μF appears to be a suitable compromise for the speed range from 0 to 60 Hz considered here for this application.

V. Numerical Simulations and Experiments

The developed numerical model of the drive was employed in simulation of dynamic behavior of the system in different transient processes. A capacitor of 20 μF was considered here. Figs. 19 to 22 present the results of simulation of sequential speed control. The supply frequency was linearly increased from 0 to 30 Hz for one-half second, for another half-second it was kept constant, and then was increased at the same rate until 57 Hz (95 % of 60 Hz) was achieved. At that moment, the full-speed mode took over and speed was maintained for another half a second. The same sequence, but in a reverse order, was applied to decrease the speed until the machine stalled.

The electromagnetic torque and mechanical speed are given in Fig. 19, the stator currents in the main and auxiliary windings in Fig 20, and the rotor currents in *d* and *q* axes are in Fig. 21. The instantaneous changeover from the full-speed mode to the reduced-speed mode and vice versa introduced brief intervals of current and torque transients. It would be possible to reduce these transients by more sophisticated timing as is shown in [11]. The overall DC-link voltage is shown in Fig. 22. The DC-link capacitors had a capacitance of 500 μF. There is a significant increase in the voltage apparent as the full-speed mode was entered. The voltage returns to its original average value after the reduced-speed

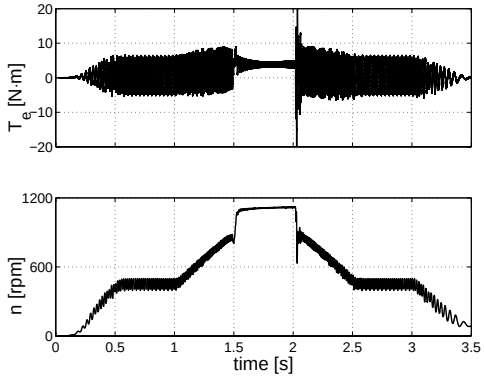

Fig. 19. Torque and speed during control of drive.

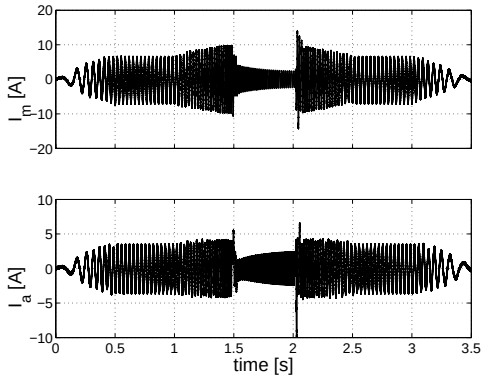

Fig. 20. Stator currents during control of drive.

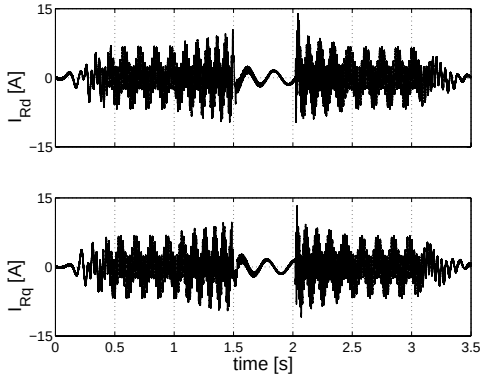

Fig. 21. Rotor currents during control of drive.

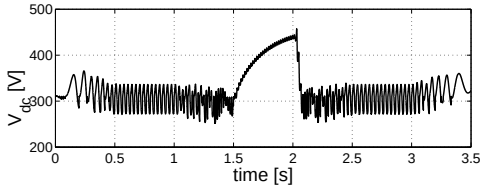

Fig. 22. DC-link voltage during control of drive.

mode is reestablished. This is caused by sudden changes in the active power delivered to the machine.

The proposed drive was built and experimentally tested in a laboratory. The results obtained agree to a great extent with the theoretical conclusions made in the preceding text.

Significant damping of the transients caused by the transition between modes was achieved by inserting suitable time delays with lengths of about 100 ms. Measured currents and voltages of the experimental drive running at half speed and loaded with corresponding torque are shown in Figs. 23 and 24. The run capacitor of 30 μF was used in this case. The high voltage at the terminals of the auxiliary winding is caused by the superposition of the voltage with the switching frequency and the voltage with the fundamental frequency and needs to be taken into account when designing a practical drive of this type. The trajectory of stator current phasor is shown in Fig. 25. The current in the auxiliary winding is multiplied by turns ratio so that the shape corresponds to the trajectory of the magnetomotive force.

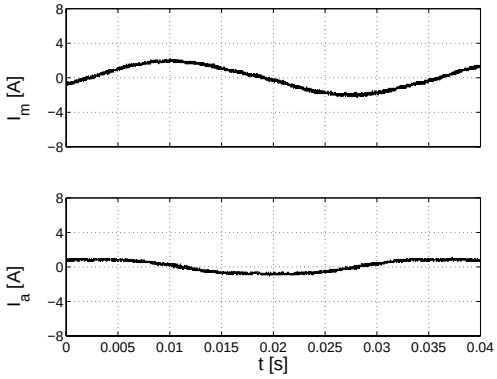

Fig. 23. Measured stator currents, f = 30 Hz, C = 30 μF.

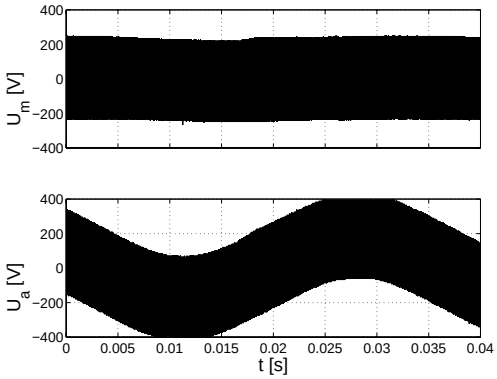

Fig. 24. Measured stator voltages, f = 30 Hz, C = 30 μF.

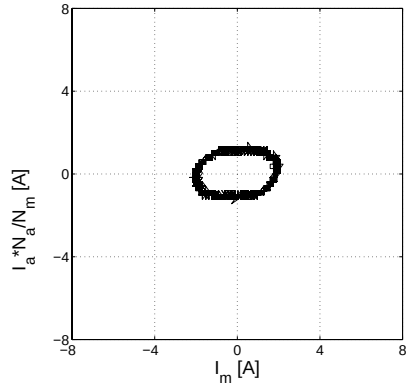

Fig. 25. Measured current trajectory, f = 30 Hz, C = 30 μF.

VI. Conclusions

The results presented in the paper suggest that the proposed drive setup could be an economically and technically viable alternative to fixed-speed and conventional variable-speed drives in many HVAC applications. The operation of the drive is not absolutely optimal throughout the entire speed range and significant torque ripple may arise in some operating points, but this should not disqualify it for most lower-power HVAC applications. A great advantage of the proposed drive is its robustness and low manufacturing cost. An increased energy efficiency should ensure a relatively quick payback of the additional investment in comparison to a fixed-speed drive. Moreover, the possibility of adjusting the mechanical speed in a broad range would provide customers with a higher level of users comfort. The prototype of the proposed drive was built and tested in a laboratory and the theoretical results obtained were proved experimentally.

ACKNOWLEDGMENT

This work was supported by the National Science Foundation under Award Number 9820434 and by the Grant Agency of the Academy of Sciences of the Czech Republic under research grant number B2057903.

REFERENCES

[1] H. N. Hickok, "Adjustable speed – a tool for saving energy losses in pumps, fans, blowers, and compressors," *IEEE Trans. on Industry Applications*, vol. 21, pp. 124-136, January/February 1985.

[2] B. A. Welchko, T. A. Lipo, "A novel variable frequency three-phase induction motor drive system using only three controlled switches," in *Conference Record IEEE Industry Applications Conference*, pp. 1468-1473, 2000.

[3] J. Klima, "Analytical model of induction motor fed from four-switch space vector PWM inverter. Time domain analysis," *Acta Technica CSAV*, vol. 44, pp. 393-410, 1999.

[4] D. G. Holmes, A. Kotsopoulos, "Variable speed control of single and two phase induction motors using a three phase voltage source inverter," in *Conference Record of IEEE/IAS Annual Meeting*, pp. 613-620, 1993.

[5] L. Julian, R. S. Wallace, P. K. Sood, "Multi-speed control of single-phase induction motors for blower applications," *IEEE Trans. on Power Electronics*, vol. 10, no. 1, pp. 72-77, January 1995.

[6] N. P. van der Duijn Schouten, B. M. Gordon, R. A. McMahon, M .S. Boger, "Integrated drives as single-phase motor replacement," in *Conference Record IEEE/IAS Annual Meeting*, pp. 922-928, 1999.

[7] M. B. R. Correa, C. B. Jacobina, A. M. N. Lima, E. R. C. da Silva, "Single-phase induction motor drives systems," in *Conference Record IEEE/APEC*, vol. 1, pp. 403-409, 1999.

[8] E. R. Benedict, T. A. Lipo, "Improved PWM modulation for a permanent-split capacitor motor," in *Conference Record IEEE Industry Applications Conference*, pp. 2004-2010, 2000.

[9] P. C. Krause, O. Wasynczuk, S. D. Sudhoff, *Analysis of electric machinery*, New York: IEEE Press, 1995.

[10] E. R. Collins, "Torque and slip behavior of single-phase induction motors driven from variable-frequency supplies, *IEEE Trans. on Industry Applications*, vol. 28, no. 3, pp. 710-715, May/June 1992.

[11] M. Chomat, T. A. Lipo, "Adjustable-speed drive with single-phase induction machine for HVAC applications," in *Conference Record IEEE/PESC*, 2001, in press.